

Shape Estimation from Topographic Primal Sketch:
an Initial Feasibility Study

Ting-Chuen Pong, Linda G. Shapiro, Robert M. Haralick

Department of Computer Science
Virginia Polytechnic Institute and State University
Blacksburg, VA. 24061

ABSTRACT

Given a gray tone image of a three-dimensional object, a topographic labeling of the image indicates the peaks and pits, ridges and valleys, and flats and hillsides of the underlying, continuous, gray tone surface. The patterns of these topographic labels capture information about the original three-dimensional object in the scene and about the illumination. In order to determine if estimation of three-dimensional shape from a topographic labeling is feasible, we have both analytically and experimentally determined the topographic labelings for images of a cylinder and a sphere with varied directions of illumination. Our results indicate that such patterns do exist and will be useful in determining three-dimensional shape from two-dimensional images.

Key words: vision, topographic labeling, shading

1. Introduction

Consider an image of a three-dimensional object illuminated by an arbitrary light source and viewed from an arbitrary position. Although ambiguities are possible, frequently the human viewer can estimate a) the three-dimensional shape of the object, b) the camera position, and c) the location of the light source. The so-called "shape-from-shading" techniques [Ho75] solve systems of differential equations to derive three-dimensional shape from gray-tone images and operate under a limiting set of restrictions. We believe that the human viewer, instead, recognizes patterns in the image that give cues leading to estimation of the shape of the object.

Extracting patterns from the original gray tone image is, in most nontrivial cases, an impossible task. In fact, it is for this reason that syntactic pattern recognition systems have had to first extract descriptions consisting of primitives, their properties, and their interrelationships from the image and then to parse these descriptions according to the rules of a grammar. Instead of trying to recognize patterns at the gray-tone intensity level, we propose to work at the topographic labeling level.

To obtain a topographic labeling, a gray tone image may be viewed as a three-dimensional continuous surface. Each point of the surface may

be labeled as part of a peak, pit, ridge, valley, saddle, hillside, or flat area. In [Ha83], these categories are defined mathematically and the topographic classification of image pixels is described. The mathematical properties of the topographic structures defined in [Ha83] are summarized in Table 1.

Table 1: Topographic Classification

| $ \nabla f $ | X_1 | X_2 | $\nabla f \cdot w_1$ | $\nabla f \cdot w_2$ | Label |
|----------------|-------|-------|----------------------|----------------------|--------------|
| 0 | -/+ | -/+ | 0 | 0 | Peak/Pit |
| 0 | -/+ | 0 | 0 | 0 | Ridge/Ravine |
| 0 | -/+ | +/- | 0 | 0 | Saddle |
| 0 | 0 | 0 | 0 | 0 | Flat |
| + | -/+ | * | 0 | * | Ridge/Ravine |
| + | * | -/+ | * | 0 | Ridge/Ravine |
| + | -,+ | 0 | -,+ | * | Hillside |
| + | -,+ | -,+ | -,+ | -,+ | Hillside |
| + | 0 | 0 | * | * | Hillside |
| + | * | * | 0 | 0 | Impossible |

where

∇f = gradient vector, $||\nabla f||$ = gradient magnitude, H = Hessian matrix, $w_i = i^{th}$ eigenvector of H , X_i = value of the second directional derivative in the direction w_i (i^{th} eigenvalue of H), and $\nabla f \cdot w_i$ = value of the first directional derivative in the direction of w_i .

Our goal is to use patterns expressed in terms of ridges and valleys, peaks and pits, flats and hillsides to estimate three-dimensional shape. In this paper, preliminary experiments employing two methods for determining such topographic patterns from gray tone intensity images of simple surfaces are described.

2. Shape from topographic patterns

There are two possible methods for determining the pattern of topographic labels that will appear, given a particular three-dimensional shape category, a particular reflectance model, a particular light source, and a particular viewpoint. The first method is to work the problem analytically, obtaining exact equations for the illuminated surface. At each point the gradient, eigenvectors, and eigenvalues can be computed in order to determine precisely which sets of points have the various topographic labels. The second method is to work the problem experimentally, using software to generate digital images of illuminated three-dimensional surfaces, to fit these image with

simple functions, and to assign topographic labels to each pixel. The first method has the advantage of exactness and the disadvantage of becoming extremely difficult for all but the simplest surfaces. The second method has the advantage of being applicable to a wide variety of surfaces and illuminating conditions and the disadvantage of yielding some inaccurate results due to possible errors in fitting the gray tone image. We have begun to experiment with both methods, starting with very simple surfaces, the Lambertian reflectance model, and point light sources. We have worked with two simple surfaces: (1) the top half of a cylinder, and (2) the upper hemisphere of a sphere. Figure 1 illustrates the two 3-dimensional surfaces.

2.1 Method 1: The Experimental Approach

The process for topographic classification can be done in one pass through the image. At each pixel of the image, the following four steps, which are discussed in more detail in [Ha83], need to be performed.

- (1) Estimate the coefficients of a cubic polynomial in a neighborhood around the pixel.
- (2) Use the estimated coefficients to find the gradient, the gradient magnitude, and the eigenvalues and eigenvectors of the Hessian at the center of the pixel's neighborhood.
- (3) Search in the direction of the eigenvectors for a zero-crossing of the first directional derivative within the pixel's area.
- (4) Recompute the gradient, gradient magnitude, and values of second directional derivative extrema at each zero crossing. Then classify the pixel based on Table 1.

2.2 Method 2: The Analytical Approach Topographic Labels on the Cylinder

Consider a cylindrical surface given by:
 $S(x,y) = d - (r^2 - y^2)^{1/2}$ for $-r \leq y \leq r$
 where d is the distance of the x - y plane from the camera down the z -axis and r is the radius of the cylinder. This surface, in which the axis of the cylinder lies along the x -axis, was chosen to simplify calculations. By differentiating S with respect to x and y , we obtain

$$S_x = 0 \text{ and } S_y = y(r^2 - y^2)^{-1/2}.$$

The intensity of the cylinder illuminated from direction (a,b,c) is given by:

$$I(x,y) = I_0 (by - c(r^2 - y^2)^{1/2}) / r$$

After some simplifications, the first and second partials of I are found to be:

$$I_x = I_{xx} = I_{xy} = I_{yx} = 0, \quad I_y = I_0 (b + cy(r^2 - y^2)^{-1/2}) / r,$$

and $I_{yy} = I_0 cr(r^2 - y^2)^{-3/2}$,
 where the subscripted I 's denote partial differentiation with respect to the subscript(s). Since I_x is equal to zero, $\|\nabla I\| = 0$ when

$$I_y = I_0 (b + cy(r^2 - y^2)^{-1/2}) / r = 0$$

$$\text{or } y^2 = r^2 b^2 / (b^2 + c^2).$$

To determine the second directional derivative extrema values and the first directional

derivatives taken in the directions which extremize second directional derivatives, we form the Hessian:

$$H = \begin{vmatrix} 0 & 0 \\ 0 & I_0 cr(r^2 - y^2)^{-3/2} \end{vmatrix}.$$

The eigenvalues of the Hessian are obtained as:

$$X_1 = I_0 cr(r^2 - y^2)^{-3/2} \text{ and } X_2 = 0;$$

their associated eigenvectors are:

$$w_1 = (0, 1) \text{ and } w_2 = (1, 0).$$

Notice that X_1 is always negative for $-r < y < r$ and $c < 0$. By taking the dot product of the gradient with the eigenvectors, we obtain:

$$\nabla I \cdot w_1 = I_y = I_0 (b + cy(r^2 - y^2)^{-1/2}) / r \text{ and } \nabla I \cdot w_2 = 0.$$

To determine the topographic labels, we need to consider two cases: (1) zero gradient magnitude and (2) positive gradient magnitude.

CASE 1: Zero Gradient Magnitude

If we let $y_0 = rb(b^2 + c^2)^{-1/2}$, then $\|\nabla I\| = 0$ when $y = y_0$. The second directional derivative extrema values at $y = y_0$ are given by

$$X_1 = I_0 cr(r^2 - y_0^2)^{-3/2} \text{ and } X_2 = 0.$$

Since X_1 is always less than zero, it follows from Table 1 that a ridge is located at $y = y_0$.

CASE 2: Positive Gradient Magnitude

If the gradient magnitude is taken to be positive, then the value of the first directional derivative in the direction of w_1 ($\nabla I \cdot w_1$) is always non-zero because $\nabla I \cdot w_1 = I_y$ and $\|\nabla I\| = |I_y|$. In this case, since X_1 is always negative and X_2 is always zero, it follows from row 7 of Table 1 that hillsides are located at those places where the gradient magnitudes are positive.

Topographic Labels on the Sphere

In the case of the sphere, the equation of a spherical surface with radius r is given by:

$$S(x,y) = d - (r^2 - x^2 - y^2)^{1/2} \text{ for } -r \leq x, y \leq r$$

Its intensity illuminated from direction (a,b,c) is given by:

$$I(x,y) = I_0 [ax + by - c(r^2 - x^2 - y^2)^{1/2}] / r$$

After some simplifications, the first and second partials of I are found to be:

$$\begin{aligned} I_x &= I_0 [a + cx(r^2 - x^2 - y^2)^{-1/2}] / r, \\ I_y &= I_0 [b + cy(r^2 - x^2 - y^2)^{-1/2}] / r, \\ I_{xx} &= I_0 c(r^2 - y^2)(r^2 - x^2 - y^2)^{-3/2} / r, \\ I_{xy} &= I_{yx} = I_0 cxy(r^2 - x^2 - y^2)^{-3/2} / r, \\ \text{and } I_{yy} &= I_0 c(r^2 - x^2)(r^2 - x^2 - y^2)^{-3/2} / r. \end{aligned}$$

The gradient magnitude ($\|\nabla I\|$) is given by:

$$\|\nabla I\| = (I_x^2 + I_y^2)^{1/2},$$

which is zero when

$$a(r^2 - x^2 - y^2)^{1/2} + cx = 0$$

and

$$b(r^2 - x^2 - y^2)^{1/2} + cy = 0$$

are satisfied simultaneously. By squaring and invoking the constraint $a^2 + b^2 + c^2 = 0$ on the unit vector (a,b,c) , the solution to the simultaneous equations is found to be:

$$x = ra \text{ and } y = rb.$$

The Hessian for the intensity surface of the illuminated sphere is given by:

$$H = \frac{I_0 c}{r(r^2 - x^2 - y^2)^{3/2}} * \begin{vmatrix} r^2 - y^2 & xy \\ xy & r^2 - x^2 \end{vmatrix}$$

Its eigenvalues are found to be:

$$X_1 = I_0 c r (r^2 - x^2 - y^2)^{-3/2}$$

$$\text{and } X_2 = I_0 c (r^2 - x^2 - y^2)^{-3/2} / r$$

Notice that both eigenvalues are always less than zero since c is always less than zero. The eigenvector corresponding to X_1 is given by:

$$w_1 = [x(x^2 + y^2)^{-1/2}, y(x^2 + y^2)^{-1/2}]$$

and the eigenvector corresponding to X_2 is given by:

$$w_2 = [-y(x^2 + y^2)^{-1/2}, x(x^2 + y^2)^{-1/2}]$$

The dot product of the gradient with w_1 is

$$\nabla I \cdot w_1 = \frac{1}{r(x^2 + y^2)^{1/2}} [x(a + \frac{cx}{(r^2 - x^2 - y^2)^{1/2}}) + y(b + \frac{cy}{(r^2 - x^2 - y^2)^{1/2}})]$$

and the dot product of the gradient with w_2 is

$$\nabla I \cdot w_2 = I_0 (-ay + bx) (x^2 + y^2)^{-1/2} / r$$

We determine the topographic labels by considering two cases.

CASE 1: Zero Gradient Magnitude

The gradient magnitude is equal to zero when $(x,y) = (ra, rb)$. Since both eigenvalues are less than zero on the illuminated sphere, it follows directly from Table 1 that a peak is located at $(x,y) = (ra, rb)$.

CASE 2: Positive Gradient Magnitude

In the case when the gradient magnitude is given to be positive, since both eigenvalues are known to be negative, it follows from Table 1 that there is a ridge at those locations where either $\nabla I \cdot w_1 = 0$ or $\nabla I \cdot w_2 = 0$ is satisfied. We obtain from above that

$$\nabla I \cdot w_1 = 0 \text{ when } (ax + by) (r^2 - x^2 - y^2)^{1/2} + c(x^2 + y^2) = 0$$

$$\text{and } \nabla I \cdot w_2 = 0 \text{ when } -ay + bx = 0$$

Table 1 also says that hillsides appear at places where both $\nabla I \cdot w_1$ and $\nabla I \cdot w_2$ are non-zero.

3. Results

In this section, we show the analytical and experimental results of the topographic patterns on the cylinder and sphere of Fig. 1. Two illumination conditions are considered for each surface: (1) the light direction is $(0,0,-1)$ which means directly above the center of the surface; (2) the light direction is $(1/2, 1/2, -1/2^{1/2})$ which translates to azimuth 45° and elevation 45° . The illuminated surfaces of the cylinder and the sphere are shown in Figure 2 and Figure 3, respectively.

3.1 Analytical Results for the Cylinder

When the light direction is from azimuth 0° , elevation 90° , analytical results in Section 2.2 indicate a ridge parallel to the axis of the cylinder and running along the center of the top half as shown in Figure 4a. When the light

direction is from azimuth 45° and elevation 45° , the ridge appears as in Figure 4b. In both cases, the remaining points of the cylinder are hillsides.

3.2 Analytical Results for the Sphere

When the light source is directly above the center of the sphere, the gradient magnitude is zero at $(0,0)$, therefore, a peak is located at the center of the sphere. The gradient magnitude is positive and the first directional derivative in the direction w_2 is zero at the remaining points of the sphere. It follows from our analytical results that ridges locate at these points.

When the light direction is $(1/2, 1/2, -1/2^{1/2})$, a peak is found at $(r/2, r/2)$. Ridges can be located at places where either

$$2^{1/2}(x^2 + y^2) = (x+y)(r^2 - x^2 - y^2)^{1/2}$$

or $x = y$ is satisfied.

At the remaining points, hillsides are the correct categories. Figure 5 shows the topographic labels for the illuminated spheres.

3.3 Experimental Results

Figures 6 and 7 show experimental results for the cylinder and sphere using cubic polynomial surface fitting. Experimental results show very good correspondence with the analytical results, except for the sphere when the light direction is $(0,0,-1)$. In this case, ridge continuums are reclassified as hillsides. A detailed discussion of ridge and valley continua can be found in [Ha83].

In addition to the images of the two simple surfaces, a synthetic image of a more complex surface was also used in testing. The surface of Figure 8 is composed of cylindrical and spherical surface patches. Figure 9 shows the image of the surface when illuminated from azimuth 45° and elevation 45° . Figure 10 illustrates the topographic labels that resulted from the experimental method. Most of the resulting topographic labels are located at places where they are predicted by the analytical method.

Our results show that the most informative features found in the images of the cylinder and sphere are ridges and peaks. While the ridges found in the cylinder images are intuitive, the ellipse-like ridges found in the sphere images are unexpected. These ellipse-like ridges will be a definite clue to 3-dimensional surface identifications. Once the shape of the surface is hypothesized as cylindrical or spherical, information such as the direction of the light source and the cylinder/sphere radius may also be estimated.

4. Conclusions

Both the analytical and experimental results so far indicate that there are definite patterns emerging that can help indicate the shape of the original three-dimensional surface and the direction of the light source. For both methods,

we anticipate a great deal more work. We would like to carry out the analytic approach for several more simple surfaces. For the experimental methods, we need to work on getting results as close as possible to the analytic results. We will then perform a large series of experiments with various surfaces, combinations of surfaces forming objects, viewpoints, reflectance functions, and lighting conditions. Only then will we be able to begin the work of analyzing the patterns of topographic labels produced and predicting three-dimensional shape from these patterns.

Bibliography

- Horn, B.K.P., "Obtaining Shape from Shading Information," *The Psychology of Computer Vision*, P.H. Winston (ed.), McGraw-Hall, New York, 1975, pp.115-155.
- Haralick, R.M, L.T. Watson and T.J. Laffey, "The Topographic Primal Sketch," *The International Journal of Robotics Research*, Vol. 2, No. 1, 1983, pp.50-72.

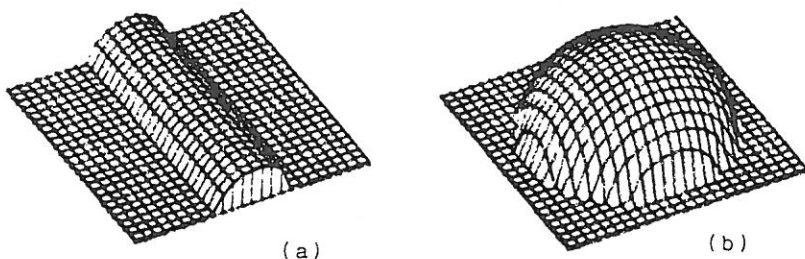


Figure 1: (a) the top half of a cylinder and (b) the upper hemisphere of a sphere.

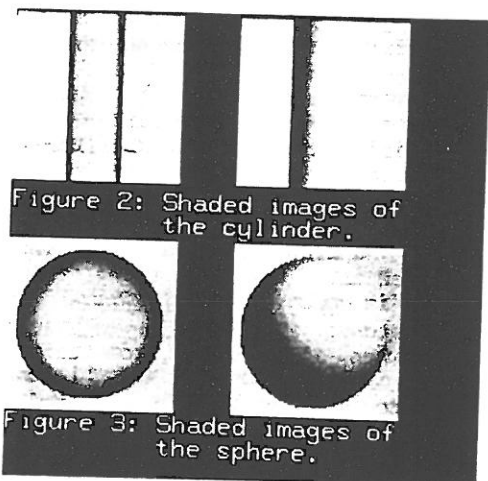


Figure 2: Shaded images of the cylinder.

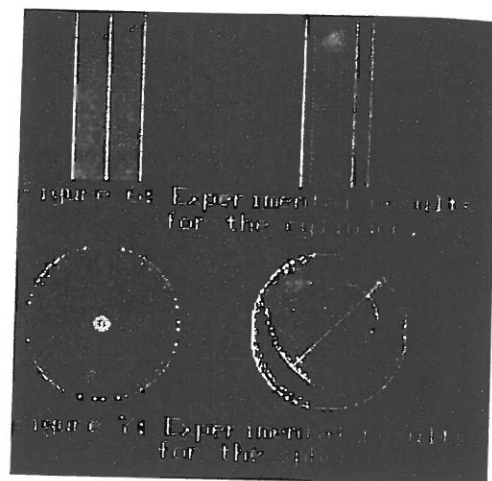


Figure 3: Experimental results for the cylinder.

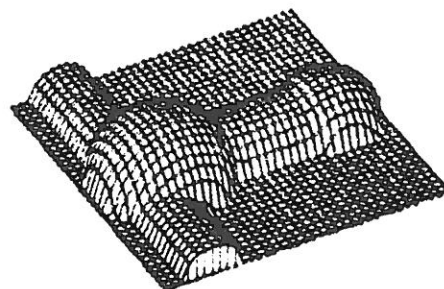


Figure 8: a synthetic 3-dimensional object.

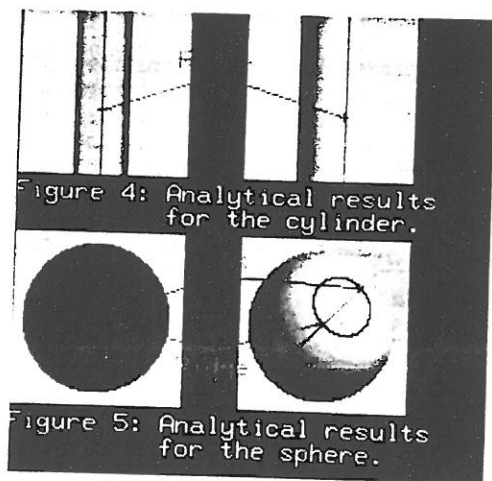


Figure 4: Analytical results for the cylinder.

Figure 5: Analytical results for the sphere.

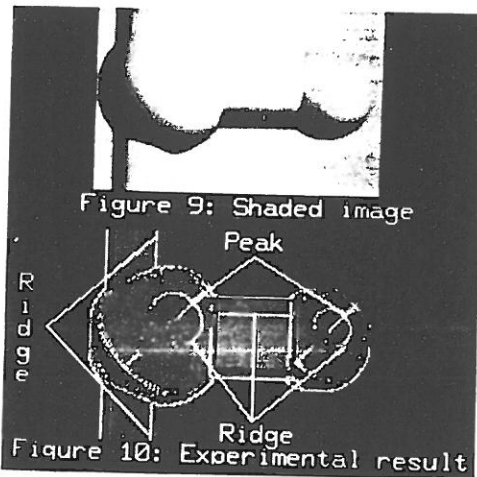


Figure 9: Shaded image

Figure 10: Experimental result